Regulation of cysteine-rich protein 2 localization by the development of actin fibers during smooth muscle cell differentiation

Takanori Kihara[1]*, Satoko Shinohara[1], Risa Fujikawa[1], Yasunobu Sugimoto[1], Masayuki Murata[2], and Jun Miyake[1]

[1]*Department of Mechanical Science and Bioengineering, Graduate School of Engineering Science, Osaka University, 1-3 Machikaneyama, Toyonaka, Osaka 560-8531, Japan*

[2]*Department of Life Sciences, Graduate School of Arts and Sciences, The University of Tokyo, 3-8-1 Komaba, Meguro-ku, Tokyo 153-8902, Japan*

*Corresponding author. Phone: +81 6 6850 6550, Fax: +81 6 6850 6557.

E-mail address: takanori.kihara@gmail.com (T. Kihara).

Abstract

Cysteine-rich protein 2 (CRP2) is a cofactor for smooth muscle cell (SMC) differentiation. Here, we examined the mechanism of CRP2 distribution dynamics during SMC differentiation. CRP2 protein directly associated with F-actin through its N-terminal LIM domain and Gly-rich region, as determined by ELISA. In undifferentiated cells that contain few actin stress fibers, CRP2 was broadly distributed throughout the whole cell, including the nucleus. After induction of SMC differentiation, CRP2 localized to actin stress fibers as they formed. The stress fiber-localized CRP2 entered the nucleus because of induced actin depolymerization. These CRP2 dynamics were reproduced by in silico simulation. CRP2 localization dynamics, which affect CRP2 function, are regulated by the formation of actin stress fibers in conjunction with SMC differentiation.

Keywords: CRP2; actin stress fiber; nuclear localization; smooth muscle cell differentiation; in silico simulation

Abbreviations used: *CRP2, cysteine-rich protein 2; SMC, smooth muscle cell; SRF, serum response factor; MRTF, myocardin-related transcription family; F-actin, filamentous actin; G-actin, globular actin; CLSM, confocal laser scanning microscope; FLIP, fluorescence loss in photobleaching; RA, retinoic acid; EMT, epithelial-to-mesenchymal transformation*

1. Introduction

Cysteine-rich proteins (CRPs; also referred to as CSRPs) are reported to be related to muscle cell differentiation [1-5]. CRPs consist of 2 LIM domains and 2 glycine-rich regions. The LIM domain is a double zinc-finger-like structure that mediates protein-protein interactions. Four members of the CRP family (CRP1, CRP2/SmLIM, CRP3/MLP, and TLP) have been identified in vertebrates; these members share a high degree of sequence homology with each other (reviewed in [6]). The gene expression patterns of these family members differ; moreover, vascular smooth muscle cells (SMCs) express CRP1 and CRP2 [7-9], which act as cofactors for SMC differentiation. CRP1 and CRP2 associate with serum response factor (SRF) and GATA proteins, forming SRF-CRP1/2-GATA complexes that strongly activate SMC-specific gene targets [4]. Furthermore, CRP2 acts as a potent transcriptional co-adaptor that remodels silent SMC gene chromatin and activates gene expression [10].

CRP2 localizes to cell nuclei, as well as to the cytoplasm, where it associates with the actin cytoskeleton [4,11]. In chick embryo proepicardial cells, endogenous CRP2 localizes to the nucleus, but CRP2 translocates the cytoskeleton as these cells fully differentiate into SMCs [4]. Although the translocation mechanism of CRP2 during SMC differentiation is unclear, it is thought that CRP2 plays different roles in these different locations. In the nucleus, as mentioned above, CRP2 acts as a transcriptional regulator of SRF-dependent SMC genes [4,10]. In the cytoplasm, the distinct role of CRP2 is unclear, but CRP2 may be involved in the assembly and maintenance of the actin cytoskeleton. CRP2 directly associates with actin filaments, α-actinin, and zyxin in vitro [8,11]. CRP1 also directly associates with actin filaments both in vitro and in vivo and stabilizes actin filament formation in vitro [12,13].

Coronary SMC differentiation requires Rho GTPase-mediated actin cytoskeleton reorganization [14]. Actin polymerization closely correlates with the activation of the nucleosomal SRF-dependent SMC genes through the regulation of localization of the members of the myocardin-related transcription family (MRTF), MKL1 and MKL2 [15-17]. Therefore, the role of multifunctional CRP2 in actin cytoskeleton organization during SMC differentiation remains to be clarified. In this study, we focused on the dynamics of CRP2 localization, which affects CRP2 function, and examined these dynamics with respect to actin stress fiber formation.

2. Materials and methods

2.1. Materials

P19CL6 cells were obtained from RIKEN Bioresource Center (Ibaraki, Japan). A7r5 cells were obtained from DS Pharma Biomedical Co. Ltd (Osaka, Japan). LipofectAMINE Plus was purchased from Invitrogen (Carlsbad, CA). FuGENE 6 was purchased from Roche Diagnostics (Basel, Switzerland). The mouse kidney cDNA library, pEGFP-C1 vector, and TALON metal-affinity resin were purchased from Clontech (Mountain View, CA). The pET28b vector was purchased from Merck KGaA (Darmstadt, Germany). Actin protein (from Bovine skeletal muscle), cytochalasin D, latrunculin B, anti-$(His)_6$ tag antibodies, and anti-SM α-actin antibodies were purchased from Sigma-Aldrich (St. Louis, MO). *Escherichia coli* BL21(DE3)pLysS were purchased from Takara Bio Inc. (Shiga, Japan). B-PER, Halt protease inhibitor cocktail (EDTA-free), and BCA protein assay kits were purchased from Thermo Fisher Scientific Inc. (Rockford, IL). Cell Illustrator software version 5.0 was purchased from GNI (Tokyo, Japan). Other reagents were purchased from

Wako Pure Chemical Industries Ltd. (Osaka, Japan), Sigma-Aldrich, Invitrogen, or Takara Bio Inc.

2.2. Plasmid construction

The mouse *Crp2* gene was amplified from the mouse kidney cDNA library by PCR, and the amplified fragment was cloned. Thereafter, the locus was subcloned into the pEGFP-C1 vector, and the finished product was named pEGFP-Crp2. In addition, the locus was subcloned into the pET28b vector by using *Nco*I and *Xho*I restriction sites. This construct encodes a $(His)_6$ tag at the C-terminus of Crp2; this construct was named pET28-Crp2. The N-terminal LIM domain and glycine-rich region (N-(LIM/G); 1–82 amino acid) and the C-terminal LIM domain and glycine-rich region (C-(LIM/G); 118–192 amino acid) of Crp2-encoding plasmids were generated from pET28-Crp2 by PCR and were named pET28-NLIM and pET28-CLIM, respectively.

2.3. Expression and purification of recombinant proteins

E. coli BL21(DE3)pLysS were transformed with pET28-Crp2, pET28-NLIM, or pET28-CLIM. LB media, supplemented with 0.5 mM IPTG, was inoculated with transformed *E. coli* in the growth phase and cultured at 30 °C for 4 h. The cells were harvested and lysed with a lysis buffer B-PER, containing an EDTA-free Halt protease inhibitor cocktail and 1.5 U/mL DNase I. The resulting lysate was sonicated and centrifuged. The supernatant was applied to a TALON Metal Affinity resin column. After serial washes with a wash buffer (10 mM Tris-HCl (pH 7.5) containing 150 mM NaCl and 0.1% TritonX-100) supplemented with 10 mM imidazole, the CRP2 protein bound to the resin through its $(His)_6$ tag and was subsequently eluted with wash buffer

containing 100 mM imidazole. The eluted protein was then dialyzed. The dialyzed protein was collected, and the concentration was determined with a BCA protein assay kit. Purified and quantified CRP2, N-(LIM/G), and C-(LIM/G) were analyzed by 16.5% SDS-PAGE.

2.4. CRP2 binding assay

The binding activity of CRP2, N-(LIM/G), or C-(LIM/G) to actin proteins was determined by ELISA. Filamentous actin (F-actin) and globular actin (G-actin) were prepared from bovine actin protein. F-actin was formed by incubating actin protein (0.48 μM) with F-buffer (5 mM Tris-HCl (pH 8.0), 100 mM KCl, 2 mM $MgCl_2$, 0.2 mM $CaCl_2$, 1 mM ATP, 0.5 mM DTT) and 1.44 μM phalloidin at 37 °C for 120 min. G-actin was prepared by incubating with actin protein (0.48 μM), G-buffer (5 mM Tris-HCl (pH 8.0), 0.2 mM $CaCl_2$, 0.2 mM ATP, 0.5 mM DTT), and 1.44 μM cytochalasin D or 1.44 μM latrunculin B at 37 °C for 120 min. The prepared actin proteins (0.48 μM) were adsorbed onto a 96-well ELISA plate. After blocking with 1% BSA, recombinant CRP2 proteins were added and allowed to react with the actin proteins at 4 °C overnight. The plate was incubated with mouse anti-$(His)_6$ tag antibodies at 30 °C for 3 h and subsequently with peroxidase-conjugated anti-mouse IgG antibodies for 90 min. The immunoreactivities were assayed using a TMB solution. The TMB reaction was stopped by sulfuric acid, and absorbance at 450 nm was measured.

2.5. Cell culture, transfection, and photobleaching

P19CL6 cells were cultured in α-MEM supplemented with 10% FBS and antibiotics.

A7r5 cells were cultured in DMEM supplemented with 10% FBS and antibiotics. P19CL6 cells were transfected using FuGENE 6; A7r5 cells were transfected using LipofectAMINE Plus reagents, as recommended by the manufacturers. The transfected cells were observed by confocal laser scanning microscopy (CLSM; LSM510, Carl Zeiss or FV1000, Olympus). In fluorescence loss in photobleaching (FLIP) assay, a small region of the cytoplasm of the EGFP-CRP2-expressing living cell was bleached with the maximum powered laser. Cell scanning and bleaching were carried out alternately at 2 sec intervals by CLSM.

2.6. Fluorescence staining

Cells were fixed with 4% paraformaldehyde, permeabilized with 0.5% Triton X-100, and blocked with 3% BSA. They were then incubated in rhodamine-labelled phalloidin and DAPI or mouse anti-SM α-actin and subsequently with Cy3-labelled anti-mouse IgG. The specimens were observed with CLSM.

2.7. In silico simulation

CRP2 dynamics during SMC differentiation were simulated in silico by using Cell Illustrator software. The software is based on a hybrid functional Petri net system [18]. Because the purpose of the simulation was validation of CRP2 dynamics in silico, we manually tuned the parameters for the speed of processes and contents of elements corresponding to our experiments. The volume ratio of nucleus:cytoplasm was set as 1:3.

3. Results

3.1. Actin-binding activity of CRP2

From previously reported co-sedimentation assays, CRP2 directly binds F-actin [11]. However, the co-sedimentation assays have not clarified whether CRP2 associates with G-actin. Initially, we used ELISA to evaluate the binding activity of CRP2 to both G-actin and F-actin in vitro. CRP2 clearly bound F-actin in the ELISA assay, and thus, the K_{off} of the complex was very low (Fig. 1a). The apparent K_d between CRP2 and the immobilized F-actin was approximately 57 nM. On the other hand, CRP2 partly bound G-actin (cytochalasin D-treated or latrunculin B-treated actin), and the apparent K_d between CRP2 and the immobilized G-actin was approximately 20–40 fold higher than that between CRP2 and F-actin (Fig. 1a). The actin-binding property of CRP2 is attributable to the N-terminal LIM domain and glycine-rich region (Fig. 1b), as reported for CRP1 [13]. The binding activity of N-(LIM/G) to F-actin was lower than that of the complete CRP2 protein; thus, the structure of CRP2 stabilizes the association. CRP2 easily binds to F-actin through its N-terminal LIM domain and glycine-rich region and partially interacts with monomeric actin.

3.2. Dynamics of CRP2 in vivo during SMC differentiation

The localization of endogenous CRP2 was found to shift from the nucleus to the cytoskeletal fibers during differentiation of coronary SMCs [4]. We examined the details of CRP2 dynamics during SMC differentiation by using mouse embryonic carcinoma P19CL6 cells. The P19CL6 cells were subcloned P19 cells, which differentiate into SMCs on treatment with retinoic acid (RA) [19]. P19CL6 cells were transfected with pEGFP-Crp2 and then differentiated into SMCs by RA treatment.

Undifferentiated P19CL6 cells were small and round (Fig. 2A). The EGFP-CRP2 distributed throughout the whole cell body and pericellular region in undifferentiated cells (Fig. 2A). The nuclear and cytoplasmic localizations of EGFP-CRP2 were similarly diffuse. When the cells differentiated into SMCs, they became flat, and actin stress fibers developed (Fig. 2A). This differentiation process was similar to that of the coronary SMC differentiation characteristic of epithelial-to-mesenchymal transformation (EMT) [20]. After SMC differentiation, EGFP-CRP2 clearly localized on the developing actin stress fibers (Fig. 2A).

We then analyzed the diffusion of EGFP-CRP2 in undifferentiated or SMC-differentiated cells by FLIP analysis. EGFP-CRP2 distributed in the nucleus and cytoplasm of the undifferentiated cells was rapidly bleached by continuous photobleaching (Fig. 2B). On the other hand, in the SMC-differentiated cells, fluorescence of the stress fiber-bound EGFP-CRP2 remained unchanged after continuous photobleaching (Fig. 2B). It appears that CRP2 localized in the nucleus and cytoplasm diffuses freely in and out of the nucleus. Once CRP2 binds with actin stress fibers, the bound CRP2 rarely dissociates. Thus, CRP2 localization dynamics during SMC differentiation is regulated by actin stress fiber formation accompanied by EMT.

3.3. CRP2 dynamics were dominated by the actin polymerization state

To clarify the regulatory mechanism of CRP2 dynamics in SMCs, we examined the distribution of EGFP-CRP2 by depolymerizing actin fibers with cytochalasin D. In rat aortic SMC A7r5 cells, EGFP-CRP2 clearly localized at basal actin stress fibers and was barely detectable in the nucleus (Fig. 3A). When the cells were treated with

cytochalasin D, EGFP-CRP2 redistributed to the nucleus as well as the cytoplasm (Fig. 3A). The nuclear-localized EGFP-CRP2 and the nuclear/cytoplasmic localization ratio of EGFP-CRP2 clearly increased in response to actin depolymerization (Fig. 3B). Because CRP2 has a low affinity for G-actin (Fig. 1a), stress fiber-bound CRP2 would be released from actin filaments upon actin depolymerization. Owing to the increase in free CRP2 levels in the cytoplasm, the levels of the nuclear-distributed CRP2 increased. Thus, nuclear CRP2 distribution is determined by the actin polymerization state.

3.4. Simulation of CRP2 dynamics during SMC differentiation

Finally, we modelled CRP2 dynamics and actin polymerization during SMC differentiation (Fig. 4A). Tables 1 and 2 present the lists of elements (i.e., proteins and other molecules) and processes (e.g., activation, binding, and polymerization) that were modelled, respectively. All the parameters are relative values. In the model, we set EMT induction and SMC gene activity as factors that activated actin polymerization, and F-actin as an activator of SMC gene transcription via SRF activation (Fig. 4A). In the previous mRNA expression analysis during SMC differentiation, CRP2 and GATA transcripts are detectable, but SRF transcripts are undetectable in the undifferentiated proepicardial cells; and CRP2 and SRF transcripts increase during SMC differentiation, but the behavior of GATA transcripts is varied by their types [20]. We therefore allowed for the effects of SRF but excluded GATA proteins from consideration. To clarify the dynamics of CRP2 in this SMC-differentiation model, the total quantity of CRP2 was set as a constant value.

In the undifferentiated condition, the value of EMT induction (process no. 13)

was set as null. In this condition, each element converged to a stable value, and SMC gene expression was maintained at a low level (Fig. 4B, Supplementary Fig. S1). The initial values for the SMC differentiation condition were then set to these converged values. By induction of SMC differentiation (setting the constant value of EMT induction), actin polymerization progressed and the amount of F-actin-CRP2 complexes increased (Fig. 4B, Supplementary Fig. S2). In the cytochalasin D treatment condition, we specified actin to be in a depolymerized state (changed parameter no. 3 and no. 4). The F-actin-CRP2 disappeared, and cytoplasm- and nuclear-distributed CRP2 levels increased (Fig. 4B, Supplementary Fig. S3). These results are in accord with our experimental results, and thus, the regulatory mechanism of CRP2 dynamics can be interpreted from our model.

4. Discussion

In this study, we clarified that CRP2 dynamics are regulated by the development of actin stress fibers during SMC differentiation. CRP2 that is distributed throughout the entire cell in the case of undifferentiated cells localizes to developing actin stress fibers during SMC differentiation (Fig. 2). This translocation mechanism is based on the direct association between CRP2 and F-actin (Fig. 1). Our data suggest that the reorganization of the actin cytoskeleton is able to affect the progress of SMC differentiation through not only SRF activation but also CRP2 translocation. In progenitor cells, CRP2 is distributed throughout the nucleus and the cytoplasm (Fig. 2); however, SRF transcripts are present at a low level [20] such that CRP2 weakly activates nucleosomal SMC genes. As actin stress fibers develop, nuclear and

cytoplasmic CRP2 localizes to these fibers (Fig. 3), and SRF transcript levels increase [20]. The remaining nuclear CRP2 contributes to SMC gene activation through complex formation with SRF and GATA proteins. This contribution may be restricted but assist the SMC differentiation. Furthermore, when actin stress fibers are reduced for any reason during the progression of SMC differentiation (e.g., loss of mechanical tension from outside or EMT inhibition), actin-bound CRP2 could release from actin fibers, enter the nucleus, and enhance SMC gene activation. On the otherhand, cytoplasmic CRP2 may stabilize actin bundle formation, as suggested for CRP1 [12], and may inhibit environmental alteration-induced reorganization of stress fibers [11]. Considering the stable association between the CRP2 and F-actin (Fig. 1, 2), the affects of cytoplasmic CRP2 for F-actin become more important for SMC differentiation. We therefore speculate that actin-bound CRP2 plays both direct and indirect roles in the stabilization of SMC differentiation.

Differentiation of SMCs requires actin cytoskeleton reorganization [14]. Particularly, actin polymerization dynamics regulate the activities of the powerful SMC gene activators MKL1 and MKL2 [21,22]. They bind G-actin and translocate into the nucleus in response to actin polymerization [16,23,24]. One of the inducers of SMC differentiation caused by actin reorganization will therefore be MKL1 and MKL2. On the other hand, CRP2 translocation is also regulated by the actin reorganization, in a direction opposite to that of MKL1/2. CRP2 may stabilize SMC differentiation and maintain the differentiated phenotype as described above. Future studies will address the interrelationship of these factors in the process of SMC differentiation and phenotype maintenance.

Acknowledgements

This work was supported by grants from the Graduate School of Engineering Science, Osaka University (Multidisciplinary Research Laboratory System to T.K.) and from Okinawa prefecture (Research project of industrialization of Medical Innovation and Technology to J.M.).

References

[1] S. Arber, G. Halder, P. Caroni, Muscle LIM protein, a novel essential regulator of myogenesis, promotes myogenic differentiation. Cell 79 (1994) 221-231.

[2] S. Arber, J.J. Hunter, J. Ross, Jr., et al., MLP-deficient mice exhibit a disruption of cardiac cytoarchitectural organization, dilated cardiomyopathy, and heart failure. Cell 88 (1997) 393-403.

[3] M.K. Jain, S. Kashiki, C.M. Hsieh, et al., Embryonic expression suggests an important role for CRP2/SmLIM in the developing cardiovascular system. Circ Res 83 (1998) 980-985.

[4] D.F. Chang, N.S. Belaguli, D. Iyer, et al., Cysteine-rich LIM-only proteins CRP1 and CRP2 are potent smooth muscle differentiation cofactors. Dev Cell 4 (2003) 107-118.

[5] J.F. Sagave, M. Moser, E. Ehler, et al., Targeted disruption of the mouse Csrp2 gene encoding the cysteine- and glycine-rich LIM domain protein CRP2 result in subtle alteration of cardiac ultrastructure. BMC Dev Biol 8 (2008) 80.

[6] R. Weiskirchen, K. Gunther, The CRP/MLP/TLP family of LIM domain proteins: acting by connecting. Bioessays 25 (2003) 152-162.

[7] M.K. Jain, K.P. Fujita, C.M. Hsieh, et al., Molecular cloning and characterization of SmLIM, a developmentally regulated LIM protein preferentially expressed in aortic smooth muscle cells. J Biol Chem 271 (1996) 10194-10199.

[8] H.A. Louis, J.D. Pino, K.L. Schmeichel, P. Pomies, M.C. Beckerle, Comparison of three members of the cysteine-rich protein family reveals functional conservation and divergent patterns of gene expression. J Biol Chem 272 (1997) 27484-27491.

[9] J.R. Henderson, T. Macalma, D. Brown, J.A. Richardson, E.N. Olson, M.C. Beckerle, The LIM protein, CRP1, is a smooth muscle marker. Dev Dyn 214 (1999) 229-238.

[10] D.F. Chang, N.S. Belaguli, J. Chang, R.J. Schwartz, LIM-only protein, CRP2, switched on smooth muscle gene activity in adult cardiac myocytes. Proc Natl Acad Sci U S A 104 (2007) 157-162.

[11] M. Grubinger, M. Gimona, CRP2 is an autonomous actin-binding protein. FEBS Lett 557 (2004) 88-92.

[12] T.C. Tran, C. Singleton, T.S. Fraley, J.A. Greenwood, Cysteine-rich protein 1 (CRP1) regulates actin filament bundling. BMC Cell Biol 6 (2005) 45.

[13] H.S. Jang, J.A. Greenwood, Glycine-rich region regulates cysteine-rich protein 1 binding to actin cytoskeleton. Biochem Biophys Res Commun 380 (2009) 484-488.

[14] J. Lu, T.E. Landerholm, J.S. Wei, et al., Coronary smooth muscle differentiation from proepicardial cells requires rhoA-mediated actin reorganization and p160 rho-kinase activity. Dev Biol 240 (2001) 404-418.

[15] C.P. Mack, A.V. Somlyo, M. Hautmann, A.P. Somlyo, G.K. Owens, Smooth muscle differentiation marker gene expression is regulated by RhoA-mediated actin polymerization. J Biol Chem 276 (2001) 341-347.

[16] F. Miralles, G. Posern, A.I. Zaromytidou, R. Treisman, Actin dynamics control SRF activity by regulation of its coactivator MAL. Cell 113 (2003) 329-342.

[17] T. Kihara, F. Kano, M. Murata, Modulation of SRF-dependent gene expression by

association of SPT16 with MKL1. Exp Cell Res 314 (2008) 629-637.
[18] M. Nagasaki, A. Doi, H. Matsuno, S. Miyano, Genomic Object Net: I. A platform for modelling and simulating biopathways. Appl Bioinformatics 2 (2003) 181-184.
[19] R.S. Blank, E.A. Swartz, M.M. Thompson, E.N. Olson, G.K. Owens, A retinoic acid-induced clonal cell line derived from multipotential P19 embryonal carcinoma cells expresses smooth muscle characteristics. Circ Res 76 (1995) 742-749.
[20] T.E. Landerholm, X.R. Dong, J. Lu, N.S. Belaguli, R.J. Schwartz, M.W. Majesky, A role for serum response factor in coronary smooth muscle differentiation from proepicardial cells. Development 126 (1999) 2053-2062.
[21] D.Z. Wang, S. Li, D. Hockemeyer, et al., Potentiation of serum response factor activity by a family of myocardin-related transcription factors. Proc Natl Acad Sci U S A 99 (2002) 14855-14860.
[22] M.S. Parmacek, Myocardin-related transcription factors: critical coactivators regulating cardiovascular development and adaptation. Circ Res 100 (2007) 633-644.
[23] K. Kuwahara, T. Barrientos, G.C. Pipes, S. Li, E.N. Olson, Muscle-specific signaling mechanism that links actin dynamics to serum response factor. Mol Cell Biol 25 (2005) 3173-3181.
[24] M.K. Vartiainen, S. Guettler, B. Larijani, R. Treisman, Nuclear actin regulates dynamic subcellular localization and activity of the SRF cofactor MAL. Science 316 (2007) 1749-1752.

Figure legends

Fig. 1. CRP2-actin binding activity analyzed by ELISA. (a) The binding activity of CRP2 with F-actin and G-actin. G-actin was fully depolymerized by treatment with 3-fold amounts of cytochalasin D (act+CD) or with latrunculin B (act+LB). The absorbance (450 nm) of each point was calculated by subtracting the summed absorbance yielded by controls (CRP2 adsorbing to a BSA-blocked well, and a 0-nM CRP2 reaction well) from the experimental absorbance values. Values are expressed as mean ± standard deviation (n = 4). (b) The binding activity of CRP2, N-(LIM/G), or C-(LIM/G) to F-actin. Each protein was used in this assay at a concentration of 1000 nM. Values are expressed as mean ± standard deviation (n = 4).

Fig. 2. Localization dynamics of CRP2 during SMC differentiation. The P19CL6 cells were treated with 1 μM RA for 2 days to initiate SMC differentiation and cultured for another 3 days. (A) The cells were observed before (1, 3) and after (2, 4, 5) induction of SMC differentiation. The differentiated SMCs were confirmed by immunostaining with SM α-actin (5, arrowhead). Although EGFP-CRP2 was distributed throughout the whole undifferentiated cells (3, 5, arrow), it localized to the developed stress fibers in the differentiated cells (4, 5, arrowhead). (B) FLIP analysis of EGFP-CRP2 in living cells. All images in a particular row reflect the same cells. The region in the cytoplasm is indicated with a white square, and fluorescence intensity is shown in a false color code. Each row shows the fluorescence before bleaching (0 step) and after 3 consecutive repetitions of 10 bleachings (10, 20, and 30 steps). The rate constants of bleaching of target undifferentiated and SMC-differentiated cells were 0.012 (0.004) and 0.0014 (0.0012) sec^{-1}, respectively (n = 2).

Fig. 3. Dynamics of CRP2 with actin fiber conditions in A7r5 cells. (A) The EGFP-CRP2-expressing A7r5 cells were observed at basal or mid-height axial focus position. The cells were treated with or without 1 μM cytochalasin D. The distribution imparity between the nucleus and cytoplasm of EGFP-CRP2 decreased with actin depolymerization. Bar: 50 μm. (B) The fluorescence intensity and the ratios between nuclear and cytoplasmic EGFP-CRP2 were compared between the normal (Control) and cytochalasin D-treated (CD) A7r5 cells. The nuclear localization of CRP2 was significantly increased by cytochalasin D treatment. Values are expressed as mean ± standard deviation (n = 18). Statistical *t*-test analysis (2-tailed) was performed.

Fig. 4. Simulation of CRP2 localization kinetics during SMC differentiation. (A) Simulation model of kinetics of CRP2 and actin dynamics during SMC differentiation. CRP2(N) and CRP2(C) indicate nuclear and cytoplasm-distributed CRP2, respectively. (B) Schematic diagrams of the simulation results. Three different conditions were simulated: undifferentiation (undiff), SMC differentiation (SMC), and cytochalasin D treatment (CD treat). The simulation results of G-actin and CRP2 concentrations in the nucleus and cytoplasm are presented as gray scale in each cell image, and the F-actin and F-actin-CRP2 intensities are presented as line thickness in each image.

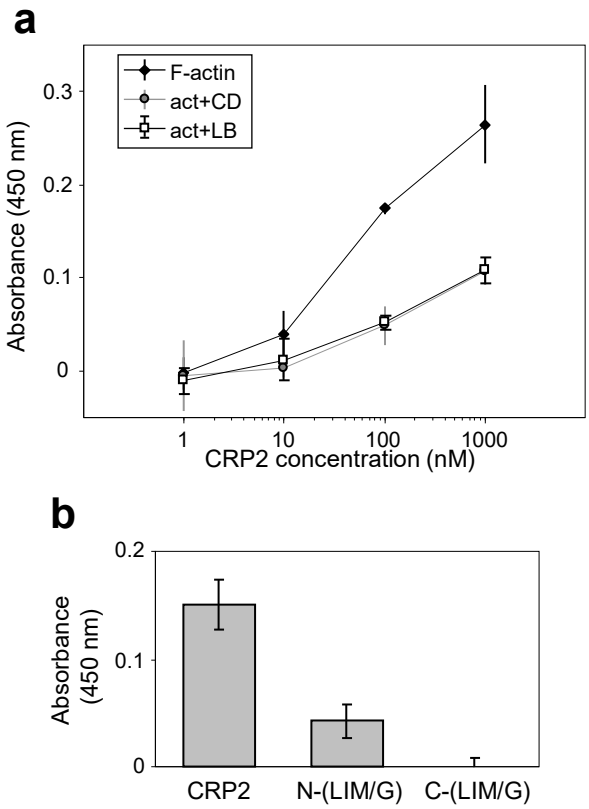

Fig.1 Kihara et al.

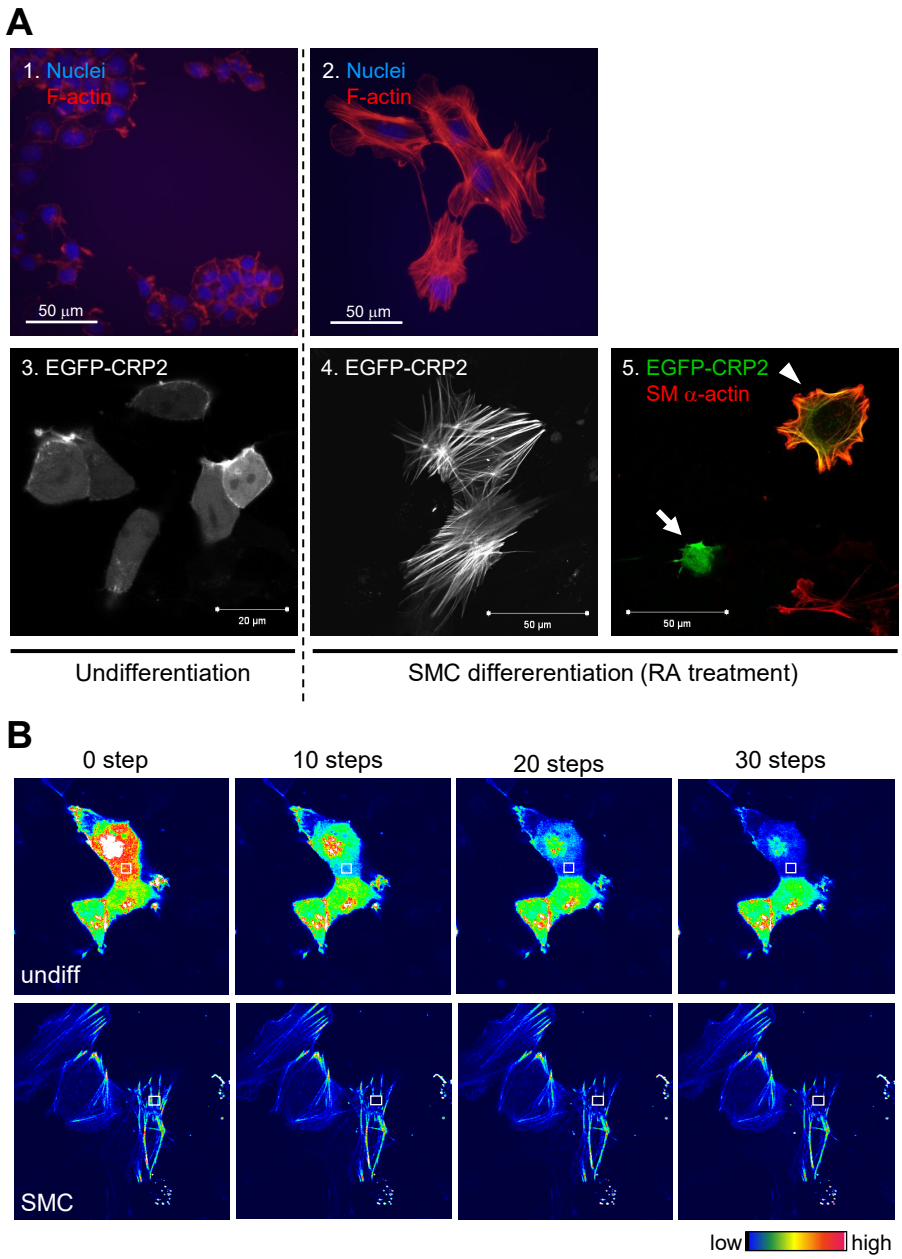

Fig. 2 Kihara et al.

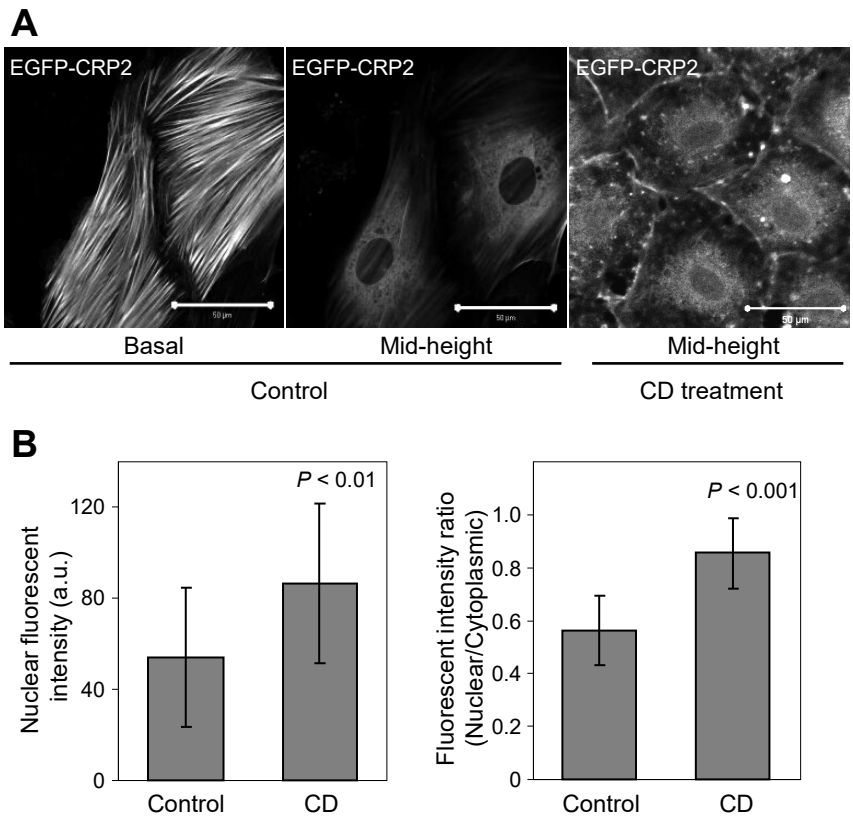

Fig. 3 Kihara et al.

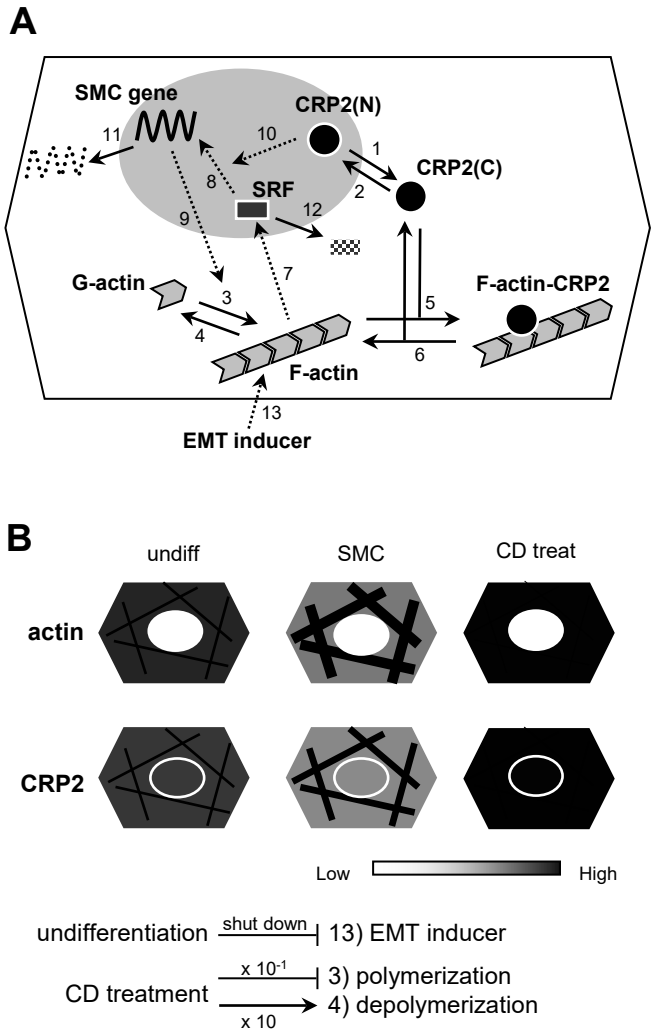

Fig.4 Kihara et al.

Table 1: Elements and their initial values of Fig. 4

Elements	Variable	Min	Max	Initial value		
				undiff	SMC	CD treat
CRP2(N)	n1	0	100	0	20	12
CRP2(C)	n2	0	100	100	59	35
G-actin	n3	0	1000	900	881	533
F-actin	n4	0	1000	100	98	414
F-actin-CRP2	n5	0	100	0	21	54
SRF	n6	0	1	0	0	1
SMC gene	n7	0	1	0	0	1
EMT inducer	n8	0	1	0.00001	1	1

Table 2: Processes and their parameters of Fig. 4

Process	Parameter	
	undiff & SMC	CD treat
1) Nuclear export	n1 * 0.3	
2) Nuclear import	n2 * 0.1	
3) Polymerization	n3 / 900	n3 / 9000
4) Depolymerization	n4 / 100	n4 / 10
5) Association	n2 * n4 / 2700	
6) Dissociation	n5 / 10	
7) Activation	n1 * 0.0001	
8) Activation	n6 * 0.01	
9) Stabilization	(n3 / 900) * (n7 * 2)	(n3 / 9000) * (n7 * 2)
10) Enhancement	(n6 * 100) * (n1 * 0.02)	
11) Degradation	0.01	
12) Degradation	0.01	
13) Enhancement	(n3 / 900) * (n8 * 4)	(n3 / 9000) * (n8 * 4)

Supplementary Figure

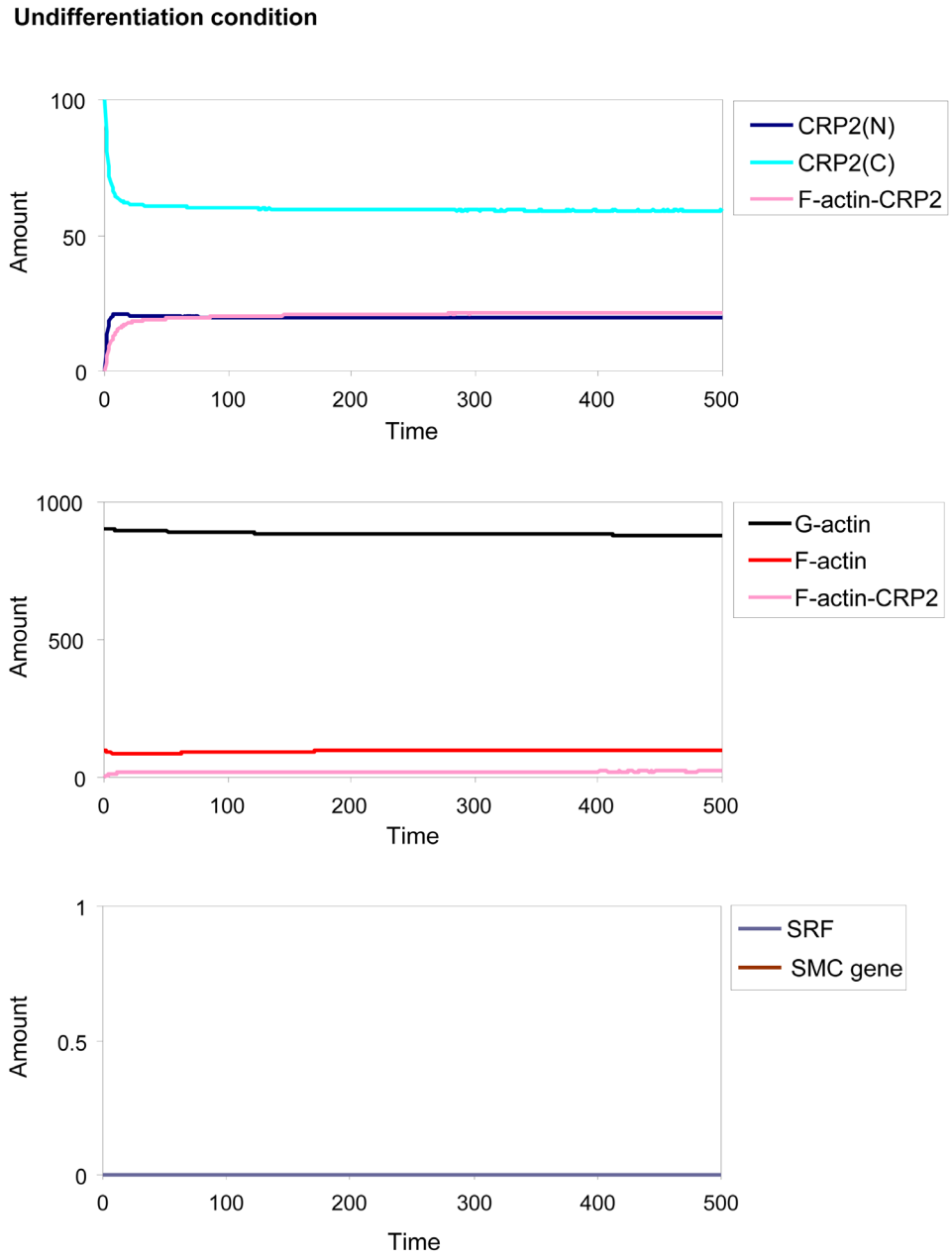

Fig. S1. The simulation results of CRP2, actin dynamics, SRF, and SMC gene expression levels in the undifferentiated condition. The Y-axis represents quantities of the components.

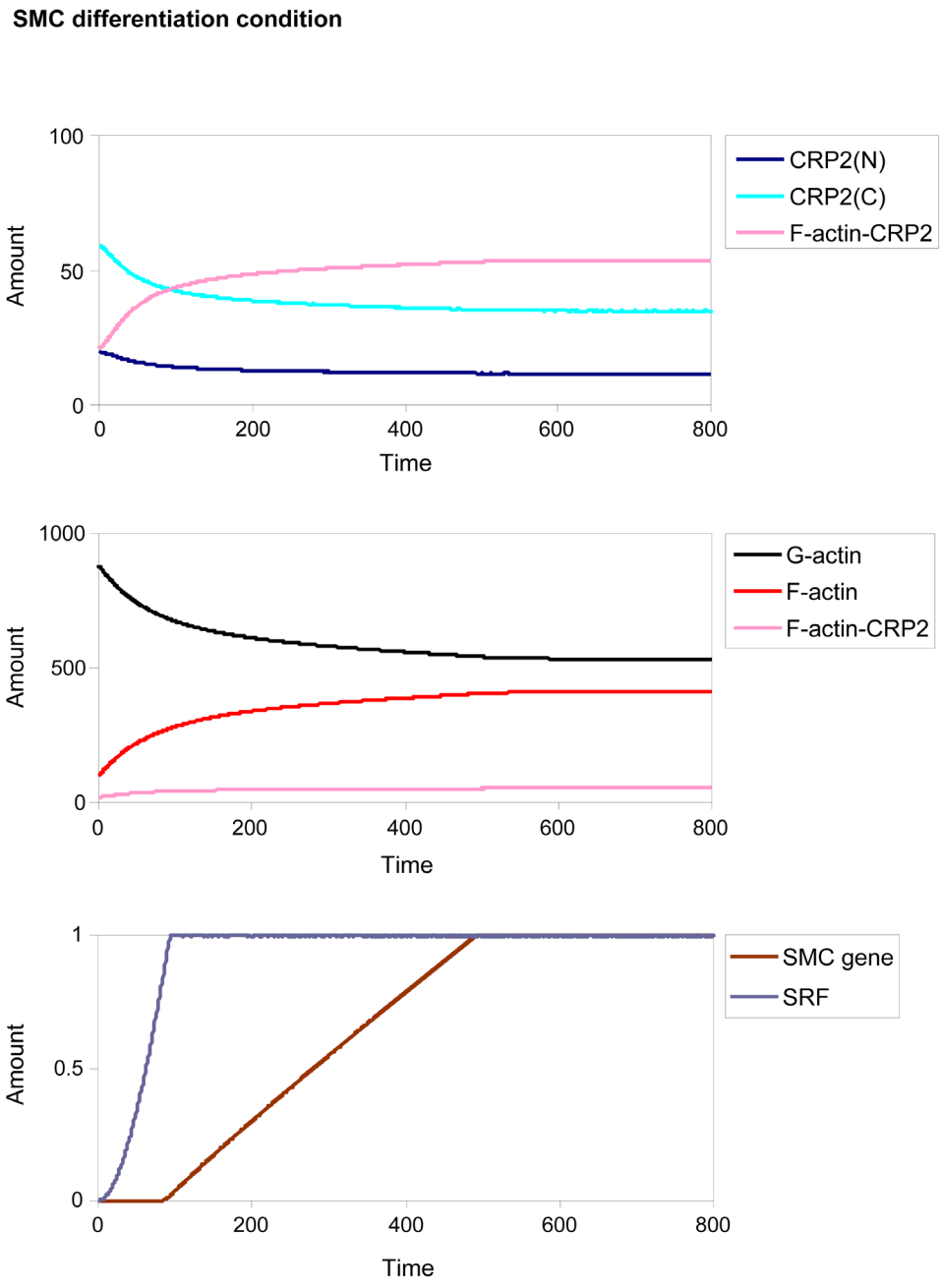

Fig. S2. The simulation results of CRP2, actin dynamics, SRF, and SMC gene expression levels in the SMC differentiated condition. The Y-axis represents quantities of the components. With EMT induction, F-actin formation increased. The increased F-actin prompted F-actin-CRP2 association and SRF activation. The activated SRF subsequently activated SMC genes.

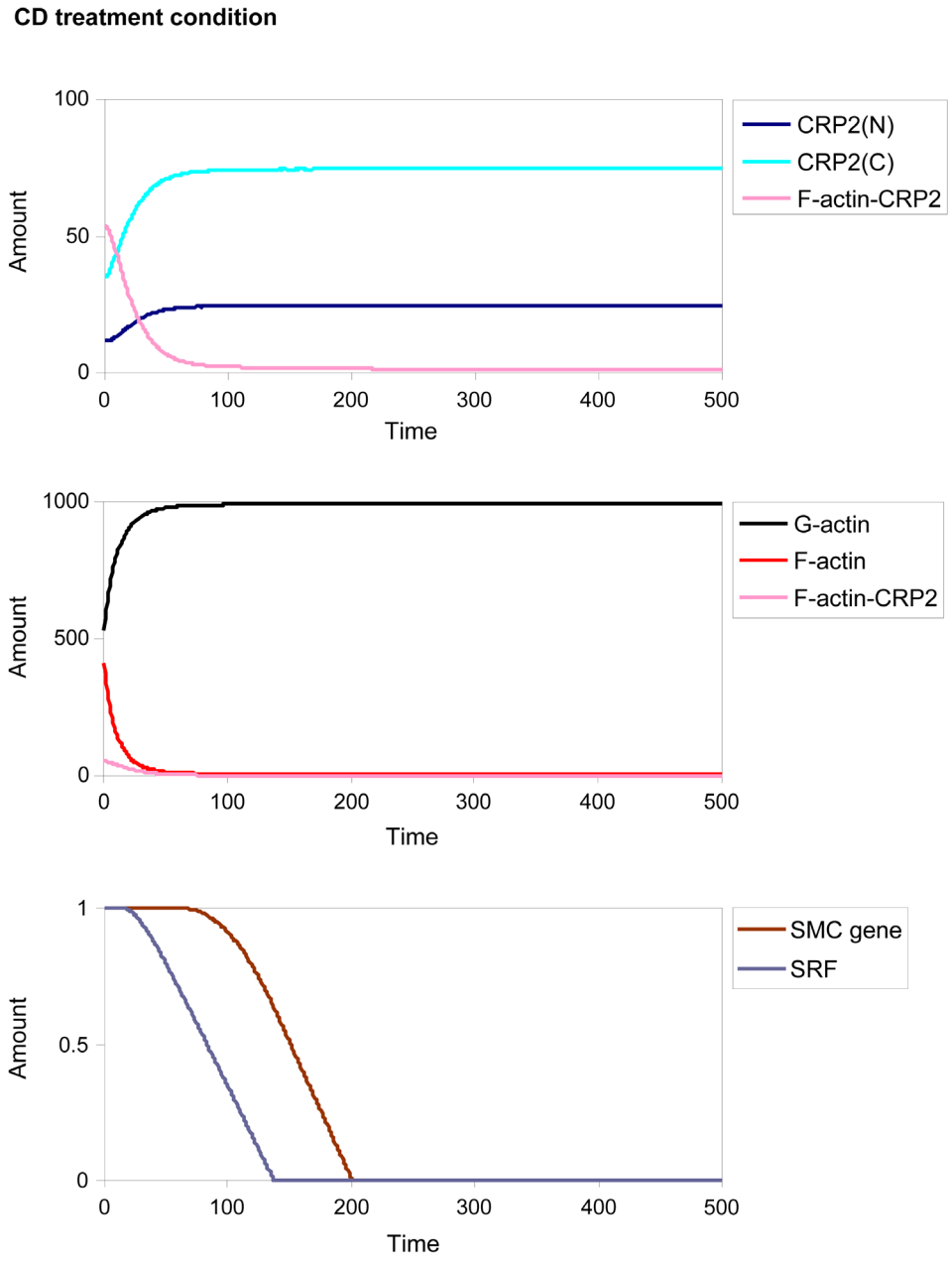

Fig. S3. The simulation results of CRP2, actin dynamics, SRF, and SMC gene expression levels in the cytochalasin D treatment condition. The Y-axis represents quantities of the components. F-actin amounts rapidly decreased, followed by dissociation of F-actin-CRP2, and an increase in nuclear CRP2. During the period of residual SRF activity, nuclear CRP2 activated and stabilized SMC gene expression.